Macromolecules

pubs.acs.org/Macromolecules Article

P(VDF-TrFE) Copolymer Dynamics as a Function of Temperature and Pressure in the Vicinity of the Curie Transition

Achilleas Pipertzis, Kamal Asadi,* and George Floudas*

Cite This: *Macromolecules* 2022, 55, 2746−2757 Read Online

ACCESS | Metrics & More | Article Recommendations | Supporting Information

ABSTRACT: We report on the phase behavior and the respective dynamics in random P(VDF-TrFE) copolymers using standard and temperature-modulated differential scanning calorimetry, X-ray diffraction, and a combination of temperature- and pressure-dependent dielectric spectroscopy measurements. Depending on the copolymer composition, the coexistence of three/four weakly ordered phases was identified in the vicinity of the Curie transition (T_c). With respect to the dynamics, we demonstrate that the segmental dynamics associated with the relaxation of constrained amorphous VDF segments at the crystal/amorphous "phase" can be used as a marker of the Curie transition. The corresponding segmental relaxation freezes at about 50 K above the lower liquid-to-glass temperature associated with the freezing of amorphous segments away from the interface. Pressure-dependent dielectric measurements provided quantitative insight into (i) the molecular origin of the segmental processes (by employing the pressure sensitivity of relaxation times and the pressure coefficient of the respective T_g's), (ii) the nature of the phase transition at T_c, and (iii) information about the stability of phases under the variation of temperature and pressure (through the $T-P$ phase diagram). We show that T_c increases linearly with pressure and is accompanied by small volume changes, implying a *weakly first-order* thermodynamic transition. Furthermore, pressure stabilizes the ferroelectric phase over a broader temperature range. This could extend the operating temperature range of ferroelectric devices based on P(VDF-TrFE) copolymers.

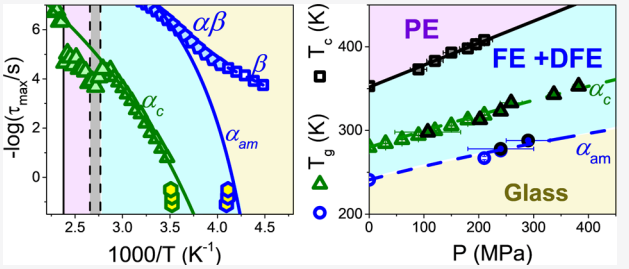

I. INTRODUCTION

Ferroelectricity is the property of polar crystals to reverse their polarity by applying a high electric field.[1] Ferroelectric polymers are of great importance for the development of organic electronics,[2,3] sensors,[4] energy storage devices,[5] power harvesting applications,[6,7] and nonvolatile memory devices.[8] Uniaxially stretched poly(vinylidene fluoride) (PVDF) and its random copolymers with trifluoroethylene (TrFE) having VDF content in the range from 50 to 80 mol % exhibit exceptional ferroelectric and piezoelectric properties.[9,10] These properties are attributed to the polar ferroelectric (FE) β-phase. Within the β-phase, the packing of molecular chains is in a planar all-trans conformation that orders all the fluorine atoms on one side of the chain and the hydrogen atoms on the other side, leading to a large spontaneous polarization.[11−14] The well-known Curie transition or Curie temperature (T_c) refers to the transition from the low-temperature FE phase to a high-temperature paraelectric (PE) phase. The latter (PE) is characterized by conformationally disordered chains, packed in a hexagonal lattice.[15] The transition from the FE to the PE phase at T_c is accompanied by (i) the disappearance of remnant polarization (in the D vs E hysteresis loop),[1,16] (ii) a maximum in the dielectric constant,[17−23] (iii) the appearance of endothermic peaks in calorimetry,[22,24] (iv) the expansion of the crystal lattice,[23−26] and (v) the weakening/disappearance of infrared absorption bands.[27]

Recent studies[28,29] reported the presence of an additional crystalline phase (the "cooled phase", CL) for copolymers with 52, 60, and 70 mol % VDF content in the vicinity of T_c. The latter (also known as DFE, i.e., the defective ferroelectric phase) is characterized by incorporating *gauche* defects in *trans* sequences.[26,28−30] Furthermore, a *relaxor* FE phase, bearing a combination of trans planar and 3/1 helical conformations, was reported in P(VDF-TrFE) copolymers with VDF content below 55%.[31−33] It was further suggested that a morphotropic phase boundary, similar to that previously found in perovskites,[35] bridges the competing FE and relaxor phases and enhances the piezoelectric properties.[31−33] The transition temperatures between the different crystalline phases are prone to copolymer composition,[22,28] processing (solvent-casting, spin-coating, etc.),[25,29,34] mechanical drawing or poling,[23−25,34] and thermal treatment.[23−25,34−36] For compositions higher than 70 mol %, it was demonstrated (i) a strong thermal hysteresis at T_c[37,38] and (ii) an approximately linear increase at T_c with pressure,[39,40]

Received: February 8, 2022
Revised: March 17, 2022
Published: March 31, 2022

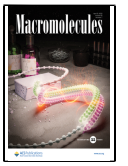

https://doi.org/10.1021/acs.macromol.2c00280
Macromolecules 2022, 55, 2746−2757

suggesting a first-order transition. For copolymers with VDF content below 70 mol %, a second-order transition was proposed based on the negligible thermal hysteresis,[31,33,37,38] whereas a first-order transition was suggested from isochronal *P*-dependent measurements.[41,42] Hence, there is an inconsistency concerning the exact order of the phase transformation at T_c for nearly equimolar compositions. Parenthetically, a second-order transition at T_c was reported for confined P(VDF−TrFE) copolymers in aluminum nanopores,[43] for terpolymers of poly(VDF-*ter*-TrFE-*ter*-CTFE),[44] and for some inorganic compounds.[45,46]

Of importance to the phase state of the copolymers and the associated molecular mobility is the presence of glass temperature(s). Well below T_c, Teyssèdre and Lacabanne[22] reported the existence of two glass temperatures (T_gs) (as with the PVDF homopolymer) by employing thermally induced current and differential scanning calorimetry measurements. The lower and higher T_gs were assigned to the freezing of the fully and constrained amorphous phases, respectively.[21] Dielectric spectroscopy can be employed to determine the composition dependence and the origin of the T_gs through the investigation of the molecular dynamics. Unfortunately, the majority of literature studies explored the dielectric properties based on isochronal temperature scans that provide only limiting information about the underlying dynamics.[19,20] Specifically, two dielectric processes—a low- and a high-temperature process associated with the noncrystalline and crystalline regions, respectively—could be assigned from the *T*-dependence of dielectric loss under isochronal conditions.[20] It was reported that the low-temperature process ($\alpha\beta$) composed of two processes with different *T*-dependencies: one with a Vogel−Fulcher−Tammann (VFT) *T*-dependence was attributed to the segmental relaxation of amorphous segments, and the one with an Arrhenius *T*-dependence was assigned to local motions.[19] The high-temperature process was attributed to cooperative motions of molecular chains into the constrained amorphous regions in the vicinity of T_c.[19,39] Evidently, for the detailed identification of the molecular dynamics in P(VDF-TrFE) copolymers, frequency-dependent measurements of the dielectric permittivity and loss are required.

Herein, we report the phase behavior and the respective dynamics in the vicinity of T_c in four P(VDF-TrFE) copolymers with PVDF/TrFE compositions (in mol %) 80/20, 75/25, 65/35, and 50/50 and their respective homopolymers by employing standard and temperature-modulated differential scanning calorimetry (DSC and TM-DSC), wide-angle X-ray scattering (WAXS), and *T*- and *P*-dependent dielectric spectroscopy measurements. Specifically, we address the following issues, only partially discussed in the literature:

- What is the exact phase behavior in the vicinity of T_c? Are there any pretransitions? To this end, depending on the copolymer composition, we report the coexistence of three/four *weakly ordered* phases in the vicinity of T_c.
- Is there a dynamic process that is linked with T_c? If so, what is its origin? Is there a discontinuous change of the molecular dynamics at T_c? By employing a combination of *T*- and *P*-dependent dielectric measurements, a strong correlation between the T_c and the α_c process, the latter related to the relaxation of constrained amorphous VDF segments at the crystal/amorphous interphase, could be identified.
- What is the nature of the T_c for P(VDF-TrFE) copolymers with lower than 70 mol % VDF content? Is it first- or second-order? What is the pressure coefficient of T_c? To this end, we report a linear $T_c(P)$ dependence for 65 mol % VDF content, implying that the transition is of the first kind.
- What is the pressure coefficient of the glass temperature(s) associated with the fully amorphous and the constrained amorphous segments?
- Can pressure be used as a tool for stabilizing certain phases? More specifically, can we stabilize the FE phase by pressure? We report that increasing pressure enhances the stability of the FE phase over a broader temperature range, which could be an asset when designing ferroelectric devices based on P(VDF-TrFE) copolymers.

II. EXPERIMENTAL SECTION

Synthesis. The two homopolymer (PVDF and PTrFE) samples and the four copolymers were purchased from Solvay. Molar masses were determined by using SEC with DMF as the eluent and with a polystyrene (PS) standard at 60 °C (three columns with porosities 1000, 1000, and 100 Å were used). Number-average molar masses (M_n) and dispersities ($Đ$) were $M_n = 1.69 \times 10^5$ g mol^{-1}, $Đ = 2.22$ and $M_n = 1.03 \times 10^5$ g mol^{-1}, $Đ = 2.72$ for PVDF and PTrFE, respectively. For the P(VDF-TrFE) copolymers, the M_n and $Đ$ values were $M_n = 1.29 \times 10^5$ g mol^{-1}, $Đ = 2.16$ for the copolymer with 80 mol % VDF content; $M_n = 1.58 \times 10^5$ g mol^{-1}, $Đ = 2.84$ for the copolymer with 75 mol % VDF content; $M_n = 1.93 \times 10^5$ g mol^{-1}, $Đ = 2.00$ for the copolymer with 65 mol % VDF content; and $M_n = 1.24 \times 10^5$ g mol^{-1}, $Đ = 2.38$ for the copolymer with 50 mol % VDF content.

Sample Preparations. For processing PVDF and P(VDF-TrFE) films, the as-received powder was placed in a manual hot press. 10−20 mg of the polymer powder was used. The compression molding was performed at temperatures ranging from 100 to 150 °C. For the compression molding process, the pressure was slowly increased up to 10 to 30 kN/cm^2. The final pressure was constant. The typical press time was 5 min. The samples were then cooled to room temperature under pressure to obtain ∼30 μm thick films. Subsequently, by using a shadow mask technique, Au electrodes, with a diameter of 10 mm, were thermally evaporated and deposited on either side of the films under a high vacuum (10^{-6} mbar). The films were subsequently used in the dielectric investigations.

Differential Scanning Calorimetry (DSC). DSC with a Q2000 (TA Instruments) was employed for the thermal properties of P(VDF-TrFE) copolymers. The temperature protocol involved measurements on cooling and subsequent heating at a rate of 2 K min^{-1} and in a temperature range between 173 and 473 K. The instrument was calibrated (including baseline calibration) for best performance in the specific temperature range and heating/cooling rate by using a sapphire standard. The enthalpy and temperature calibration were made with an indium standard ($\Delta H = 28.71$ J/g, $T_m = 428.8$ K). The heat capacity calibration was made with a sapphire standard.

In addition to normal DSC, temperature-modulated DSC (TM-DSC) measurements were performed within the temperature range from 193 to 333 K.[47,48] In TM-DSC a low-frequency sinusoidal perturbation is summarized to the standard DSC profile, according to $T = T_0 + \beta t + A_T \sin(\omega t)$, where β is the rate, t the time, A_T the amplitude, and ω the angular frequency. An amplitude of 1 K and periods in the range from 20 to 200 s with corresponding heating rates from 10 to 1 K min^{-1} have been employed. More specifically, the linear heating rate for each period of modulation was calculated from $\beta = (\Delta T/n\Pi)60$ s/min, where ΔT is the temperature width of glass "transition" (between the "onset" and "end" temperature), n is the number of modulation cycles, and Π is the period of modulation.[49] We employed six modulation cycles and seven periods of modulation (200, 150, 100, 80, 40, and 20 s).

https://doi.org/10.1021/acs.macromol.2c00280
Macromolecules 2022, 55, 2746−2757

X-ray Scattering. Wide-angle X-ray scattering (WAXS) measurements were made by using Cu Kα radiation from a RigakuMicroMax 007 X-ray generator using Osmic Confocal Max-Flux curved multilayer optics. Diffraction patterns were recorded on a 2D-detector (Mar345 Image Plate) at a sample-to-detector distance of 35 cm. Samples in the form of fibers were prepared with a mini-extruder at different temperatures. Subsequently, the fibers were inserted into glass capillaries (0.5−1 mm diameter). WAXS patterns were recorded with a vertical orientation of the filament axis and the beam perpendicular to the filament. The recorded intensity distributions were integrated along the equatorial and meridional axes and are presented as a function of the modulus of the scattering vector, $q = (4\pi/\lambda)\sin(2\theta/2)$, where λ (= 1.54184 nm) is the wavelength and 2θ is the scattering angle. Scattering curves were taken within the temperature range from 423 to 373 K in 10 K steps and from 368 to 303 K in 5 K steps on heating and subsequent cooling. Typically, 1800 s equilibration time and 1800 s measurement time at each temperature were used.

Dielectric Spectroscopy (DS). DS measurements were performed with a Novocontrol Alpha frequency analyzer. The temperature protocol of "isobaric" measurements ranged from 223 to 463 K in steps of 5 K and for frequencies in the range from 10^{-2} to 10^{7} Hz. The samples were annealed at 413 K for 2 h before the measurement. The dielectric cell for the T-dependent dielectric measurements consisted of P(VDF-TrFE) films (thickness of ~30 μm) sputtered from both sides with a gold layer of thickness of ~1 nm and a diameter of 10 mm to transform the investigated copolymers into capacitors. Measurements under hydrostatic pressure were performed in a Novocontrol pressure cell.[50] The pressure setup consisted of a T-controlled cell, hydraulic closing press with air pump, and air pump for hydrostatic test pressure. For the P-dependent measurements, the copolymers were pressed at the molten state between 20 mm diameter electrodes and Teflon spacers were used to maintain a thickness of 50 μm. Subsequently, the capacitor was wrapped with Teflon tape and placed inside a Teflon ring to prevent the flow of silicone oil (DOW CORNING 550 Fluid) into the sample. The silicone oil is the liquid that uniformly transmits the pressure to the capacitor. The isothermal measurements of relaxation times were performed with temperature stability better than 0.1 K and pressure stability better than 2 MPa. In both "isothermal" and "isobaric" measurements, the complex dielectric permittivity $\varepsilon^* = \varepsilon' - i\varepsilon''$, where ε' is the real and ε'' is the imaginary part, was obtained as a function of frequency, ω, temperature, T, and pressure, P, i.e., $\varepsilon^*(T,P,\omega)$.[51,52] The determination of relaxation dynamics was made by using the empirical equation of Havriliak and Negami (HN):[53]

$$\varepsilon^*_{HN}(\omega, T, P) = \varepsilon_\infty(T, P) + \sum_{j=1}^{3} \frac{\Delta\varepsilon(T, P)}{[1 + (i\omega\tau_{HN_j}(T, P))^{m_j}]^{n_j}} + \frac{\sigma_0(T, P)}{i\varepsilon_f\omega} \quad (1)$$

where $\varepsilon_\infty(T,P)$ is the high-frequency permittivity, $\tau_{HN}(T,P)$ is the characteristic relaxation time in this equation, $\Delta\varepsilon(T,P) = \varepsilon_0(T,P) - \varepsilon_\infty(T,P)$ is the relaxation strength, m and n (with limits $0.2 < m, mn \leq 1$) describe respectively the symmetrical and asymmetrical broadening of the distribution of relaxation times, σ_0 is the dc conductivity, and ε_f is the permittivity of free space. Assuming statistical independence in the frequency domain, a summation of two (or three) HN functions have been employed for the temperature range, where two (or three) relaxation processes coexist in the experimental window. From τ_{HN}, the relaxation time at a maximum loss, τ_{max}, is obtained analytically as follows:

$$\tau_{max} = \tau_{HN} \sin^{-1/m}\left(\frac{\pi m}{2(1+n)}\right) \sin^{1/m}\left(\frac{\pi mn}{2(1+n)}\right) \quad (2)$$

In analyzing the dynamic behavior, we have used the ε'' values at every temperature. However, in some cases, the first derivative of ε' ($d\varepsilon'/d\ln\omega \approx -(2/\pi)\varepsilon''$ has been employed for the not clearly resolved processes.

III. RESULTS AND DISCUSSION

Identification of Phase Transitions. Information about the phase behavior in the vicinity of T_c can be obtained from DSC measurements and from the T-dependence of the dielectric function, as depicted in Figures 1 and 2, respectively.

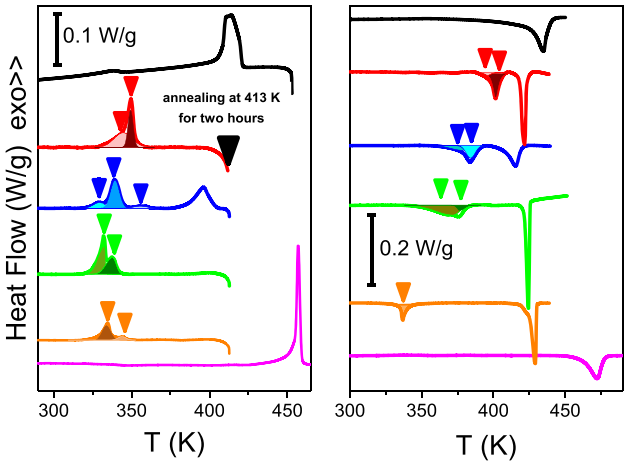

Figure 1. Standard DSC thermograms for the homopolymers; PVDF (black line) and PTrFE (magenta line) and for the P(VDF-TrFE) copolymers with different compositions, 80/20 (red line), 75/25 (blue line), 65/35 (green line), and 50/50 (orange line), upon the first cooling (left) and subsequent heating runs (right) with a rate of 2 K·min^{-1}. All copolymers were annealed at 413 K for 2 h. Traces are shifted vertically for clarity. The vertical arrows indicate multiple transitions in the vicinity of T_c (see text).

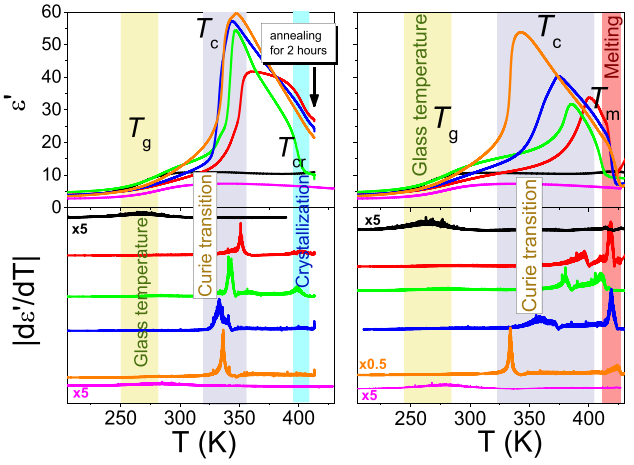

Figure 2. Temperature dependence of the dielectric permittivity, $\acute{\varepsilon}$ (top), and its first derivative with respect to temperature (bottom) for the investigated P(VDF-TrFE) copolymers with compositions 80/20 (red line), 75/25 (green line), 65/35 (blue line), and 50/50 (orange line) and their homopolymers PVDF (black line) and PTrFE (magenta line). Measurements refer to a frequency of 1×10^5 Hz with a rate of 2 K·min^{-1}, upon first cooling (left) and subsequent heating (right). The copolymers were annealed at 413 K for 2 h before the measurement.

Thermal treatment can affect the crystallinity and the exact temperature of the Curie transition.[23−25,34−36] Specifically, it was shown that annealing at temperatures above T_c results in higher crystallinity of the PE phase. Furthermore, the formation of different ferroelectric crystalline phases with different thermodynamic stability (conformational and packing defects) has been reported following annealing at temperatures below the

https://doi.org/10.1021/acs.macromol.2c00280
Macromolecules 2022, 55, 2746−2757

Table 1. Temperature and Enthalpy Change at the Curie, Cooling, and Melting Transitions during the First Cooling/Heating Run

P(VDF-TrFE)	T_c (K)	ΔH_c (J·g^{-1})	T_{cryst} (K)	ΔH_{cryst} (J·g^{-1})	T_c (K)	ΔH_c (J·g^{-1})	T_m (K)	ΔH_m (J·g^{-1})
100:0			413.9	42.5			435.0	43.4
80:20	344.6	13.1			401.7	15.9	421.8	22.4
	349.4	9.1			396.1	2.5		
75:25	329.3	3.4	396.3	16.3	377.2	7.3	415.2	14.4
	339.4	11.7			384.0	8.5		
	355.7	1.5						
65:35	332.7	9.7			372.0	17.8	424.4	
	337.8	7.9			376.6	2.7		
50:50	333.9	6.5			337.3	7.9	429.3	21.8
	343.9	1.3						
0:100			456.9	21.1			472.2	21.3

T_c.[23−25,34−36] Here, the P(VDF-TrFE) copolymers were annealed at 413 K (a temperature in the region between the Curie and melting transitions) for 2 h.[23−25,34−36]

Multiple (endothermic/exothermic) peaks associated with phase transitions can be observed in the DSC traces within the temperature range from 329 to 356 K. This region is associated with the reversible transition from the FE to the PE phase. So far, three crystalline phases have been reported at T_c: the FE, the PE, and the CL (or the DFE). For the investigated copolymers with 75 (80, 65, and 50) mol % VDF content, three (two) exothermic peaks are evident on cooling, implying the existence of four (three) different ordered phases. In addition, a thermal hysteresis that is strongly dependent on copolymer composition can be observed. The respective temperatures and enthalpy changes of the observed phase transitions are summarized in Table 1. The enthalpy change of each phase transition is extracted by fitting each endothermic/exothermic peak with a Gaussian function (Figure S1). Identical phase transitions can be observed after erasing the thermal history (Figure S2).

At higher temperatures, the DSC traces of the P(VDF-TrFE) copolymers exhibit an exothermic (endothermic) peak, corresponding to the crystallization (melting) of the system. The latter is weakly dependent on the copolymer composition and is observed at lower temperatures compared to that found in the respective homopolymers (Table 1). Interestingly, at temperatures well below T_c, the reversing heat capacity exhibits two steps during heating that correspond to two T_gs (Figure S3). In semicrystalline polymers, apart from the amorphous phase that freezes at the liquid-to-glass temperature (T_g^{low}), an additional "phase" has been identified, known as the restricted amorphous fraction (RAF) located at the crystal/amorphous interface/interphase.[54,55] The physical constraints imposed by the surrounding crystalline regions give rise to the freezing of the RAF (T_g^{high}) at higher temperatures in comparison to the fully amorphous phase. The characteristic length scale associated with T_c can be calculated by employing the Donth model as[56]

$$\xi_\alpha = \left(\frac{RT_g^2\Delta(1/C_p)}{\rho N_A(\delta T)^2}\right)^{1/3}$$

. Here, R is the gas constant, ρ (= 1.9 g cm^{-3})[57] is the density, and $\Delta(1/C_p) = 1/C_p^{glass} - 1/C_p^{liquid}$ is the inverse change of heat capacity (calculated at T_g, and $\delta T = \Delta T/2.5$ is the temperature fluctuation extracted from the width, ΔT, of the T_g range). The extracted ξ_α amounts to 1.45 (1.29) nm for the T_g^{high} (α_c) being higher than the characteristic length of the liquid-to-glass temperature which amounts to 0.92 (0.75) nm for 75 (65) mol % VDF content (Figure S4). Both the larger length of the cooperative rearranging domains and the higher T_g reflect on the nature of the RAF. Quantitative insight into the dynamics related to the two T_gs can be obtained by DS measurements (to be described in detail below).

The phase transitions in the vicinity of the Curie region have a distinct dielectric fingerprint. They can be identified by employing T-dependent measurements of the dielectric permittivity, ε', as depicted in Figure 2. An abrupt increase of ε' from a value of 10 to values in the range 40−60 is observed at T_c, reflecting changes in dipolar orientation. At higher temperatures, the dielectric permittivity decreases, during the crystallization (melting) of the copolymers, implying non-fluctuating (random-fluctuating) dipoles in the crystal (melt). The transition temperatures in the vicinity of T_c are practically independent from the applied frequency (Figure S5).

The extracted calorimetric and dielectric characteristic temperatures are summarized in the phase diagram of Figure 3. Summing up, multiple phase transitions can be observed in the vicinity of T_c, especially for the copolymer with 75 mol % VDF content, where four different ordered phases coexist in the

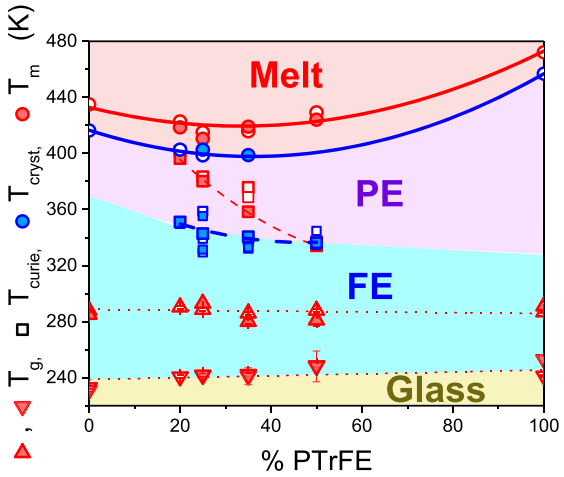

Figure 3. Phase diagram of the investigated P(VDF-TrFE) copolymers upon the first cooling (blue symbols) and subsequent heating (red symbols). Open circles and squares are extracted from thermodynamic measurements (DSC) with a rate of 2 K·min^{-1}. Filled circles and squares are obtained from isochronal dielectric measurements at a frequency of 1 × 10^5 Hz and a rate of 2 K·min^{-1}. The T_g values are obtained from TM-DSC (open triangles) and isothermal dielectric spectroscopy (filled triangles) measurements at a relaxation time of 1 s (see text). The colored areas indicate the different "phases" on cooling: melt (red), FE (cyan), PE (purple), and glassy (yellow).

https://doi.org/10.1021/acs.macromol.2c00280
Macromolecules 2022, 55, 2746−2757

vicinity of the Curie region. These transitions reflect the FE and PE phases as well as their respective defective phases.[26]

Information about the structural characteristics of the observed ordered phases in the vicinity of T_c can be obtained by WAXS measurements. WAXS patterns for the P(VDF-TrFE) copolymer with 65 mol % VDF content are depicted in Figure 4.

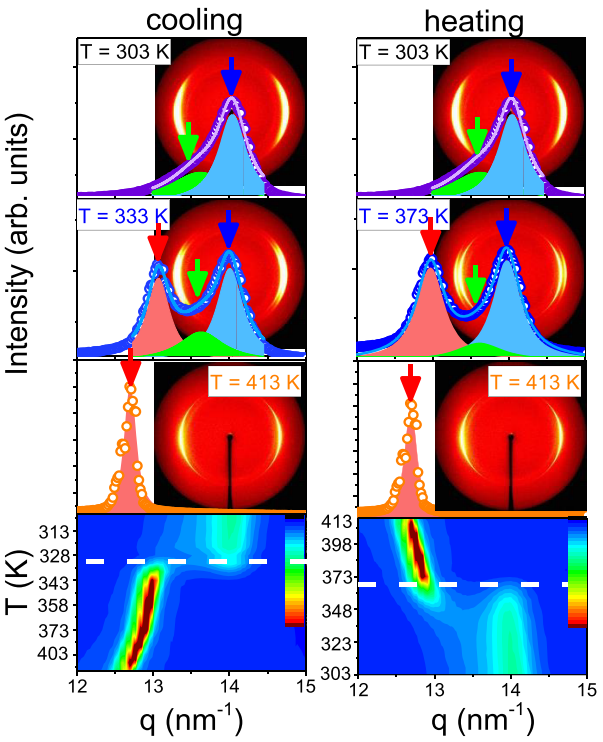

Figure 4. 2D-WAXS patterns of the P(VDF-TrFE) copolymer with composition 65/35 and intensity distribution along the equatorial axis shown at some selected temperatures, upon cooling (left) and on subsequent heating (right). The blue, green, purple, and red arrows indicate diffraction peaks corresponding to the ferroelectric (FE), defective ferroelectric (DFE), defective paraelectric (DPE), and paraelectric (PE) phases, respectively. (bottom) WAXS intensity contour plot upon cooling (left) and heating (right). The horizontal white line in the contour plot indicates the T_c.

The 2D-WAXS patterns reveal only a limited number of Bragg peaks at each phase, suggesting weakly ordered phases. As shown in Figure 4, at temperatures just below the melting point, the observed single Bragg peak corresponds to the PE phase. Approaching the T_c on cooling, the peak associated with the PE phase decreases in intensity, and two reflections appear corresponding to the FE and the defective ferroelectric phase (DFE). Hence, within the temperature range of 333 K < T < 343 K, three different phases (FE, DFE, and PE—as depicted and discussed in Figure 5) coexist in agreement with earlier studies.[26] On further cooling, the remaining part of the PE phase transforms continuously into the DFE phase. At temperatures below 328 K, the FE and DFE phases coexist. A thermal hysteresis can be observed upon subsequent heating. Multiple phase transitions were also detected in the P(VDF-TrFE) copolymer with 75/25 composition, with the only difference being the coexistence of four weakly ordered phases (FE, DFE, defective paraelectric phase (DPE), and PE) in the vicinity of T_c (Figures S6–S8).

The structural features of the different phases are compared with the calorimetric and dielectric data in Figure 5 (Figure S8)

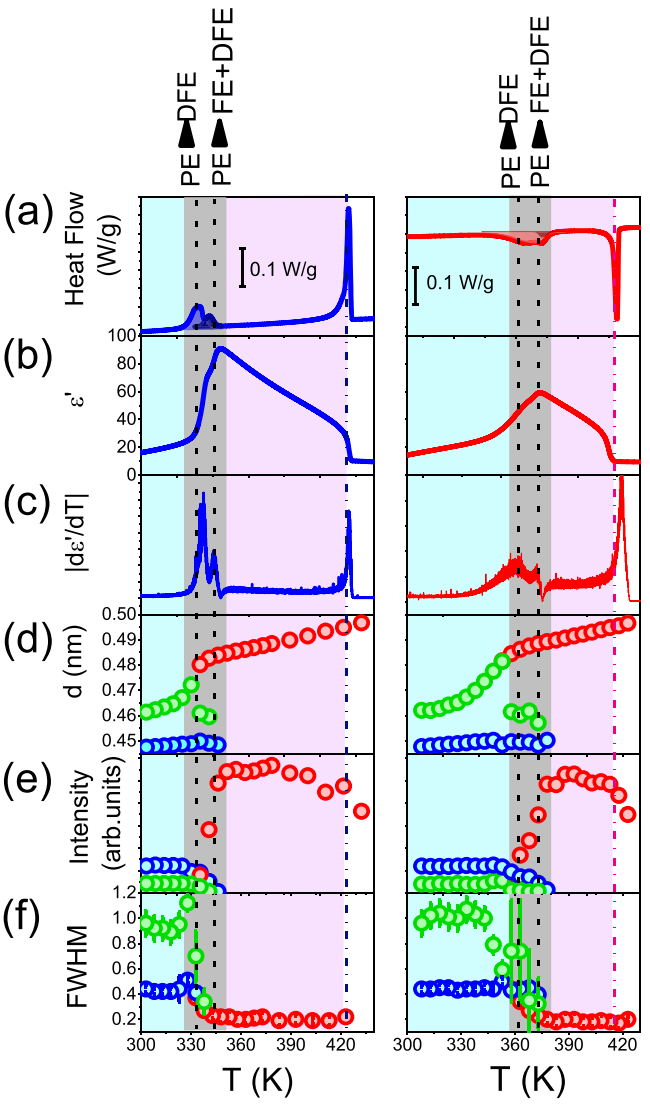

Figure 5. Temperature dependence of the (a) DSC traces (rate = 2 K·min^{-1}), (b) dielectric permittivity, $\acute{\varepsilon}$ (rate = 2 K·min^{-1}, $f \sim 1 \times 10^5$ Hz), and (c) absolute value of the first derivative of $\acute{\varepsilon}$, with respect to temperature, as well as (d) domain spacing, (e) peak intensity, and (f) full width at half-height (with uncertainties) of the most intense reflection of the PE (red symbols), DFE (green symbols), and FE (blue symbols) phase for the P(VDF-TrFE) copolymer with 65 mol % VDF content on cooling (left) and subsequent heating (right). The vertical dashed lines depict the transitions among the different ordered phases, as indicated. The red, purple, gray, and blue areas indicate the different "phases": melt state, PE, temperature range of Curie transition, and FE + DFE, respectively.

for the P(VDF-TrFE) copolymers with 65 (75) mol % VDF content. There is an excellent correlation between the thermal, dielectric, and structural features at the respective transitions (indicated with the vertical lines). All techniques probe the same (PE to DFE), (PE to FE+DFE), and (PE to melt) structural changes. The differences in the transition temperatures among X-rays, DSC, and DS results reflect the significantly smaller effective rate in the former (X-rays).

As depicted in Figure 5 (and Figure S8), the domain spacing decreases from 0.49 to 0.45 nm (0.47 nm) in going from the PE to the FE (defective phases), in accordance with previous studies.[23−26] Informative is also the comparison of the sharpness of peaks, the latter estimated from the full width at half-height of

https://doi.org/10.1021/acs.macromol.2c00280
Macromolecules 2022, 55, 2746−2757

the most intense Bragg reflection. Interestingly, the more sharp reflection appears within the PE phase, and the respective intensity is substantially higher than the one found within the FE phase for copolymers with 65 (75) mol % VDF content. However, it needs to be stressed that all phases in the vicinity of T_c are *weakly ordered* phases, suggesting that P(VDF-TrFE) copolymers comprise small crystalline lamellar structures that are interrupted by large amorphous regions.

At this point, the following questions arise: How the molecular dynamics of the copolymers influenced by the different weakly ordered phases? Is there a particular molecular process that is most affected by the Curie transition? To address these questions, we employ *T*- and *P*-dependent dielectric spectroscopy measurements.

***T*- and *P*-Dependence of Molecular Dynamics.** Precise information about the dielectrically active molecular processes and their molecular origin within the different phases can be obtained by a combination of *T*- and *P*-dependent dielectric measurements. We should point out here that the majority of literature studies refer to isochronal temperature scans, $\varepsilon'(T)$, ignoring information that can be obtained by frequency-dependent measurements of the complex dielectric function $\varepsilon^*(T,P,\omega)$. Figure 6 gives representative loss curves of the P(VDF-TrFE) copolymer with 75 mol % VDF content at some selected temperatures.

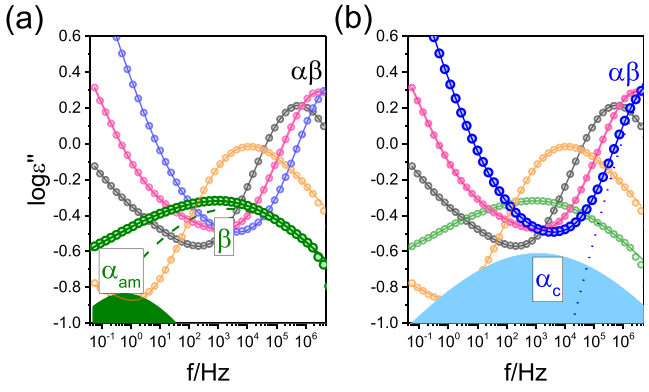

Figure 6. Dielectric loss curves for P(VDF-TrFE) copolymer with composition 75/25 at some selected temperatures: 243.15 K (olive), 263.15 K (orange), 293.15 K (black), 313.15 K (magenta), and 333.15 K (blue), obtained on heating with fitting examples shown at two temperatures: (a) The solid olive line is a fit to a summation of two HN functions at 243.15 K. The olive shadowed area and the dashed line indicate simulations of the α_{am} and β processes, respectively (see text). (b) The solid blue line represents a fit to a summation of two HN functions in addition to the dc-conductivity contribution at 333.15 K. The shadowed blue area and the dotted line indicate simulations of the α_{am} and $\alpha\beta$ processes, respectively (see text).

The P(VDF-TrFE) copolymers exhibit four dielectrically active processes, termed β, α_{am}, $\alpha\beta$, and α_c. Each process can be described by a single HN function (Figure 6). The extracted low (m) and high (mn) frequency slopes of the different processes as well as the effective dielectric strength, $T\Delta\varepsilon$, are listed in Table S2. At lower temperatures, the local β process is followed by the α_{am} process, associated with the segmental relaxation of the fully amorphous phase. The freezing of the α_{am} process defines the lower liquid-to-glass temperature, T_g (low T_g in DSC). The presence of a single segmental process in the copolymers related to the fully amorphous phase (despite the presence of both VDF and TrFE amorphous segments) is attributed to their random distribution along the chain and to the proximity of the glass-to-liquid temperatures of the parent homopolymers (Figure S9). Indeed, in the copolymers a single α_{am} is found intermediate to the respective homopolymers. At higher temperatures, the α_{am} and β processes merge to form the $\alpha\beta$ process, with increasing effective dielectric strength ($T\Delta\varepsilon^{\alpha\beta} \sim T\Delta\varepsilon^{\alpha_{am}} + T\Delta\varepsilon^{\beta}$, also listed in Table S2). Similar merging of the α_{am} and β processes was evidenced in, for example, poly(ethyl methacrylate).[58] A slower process (termed α_c) in comparison to the $\alpha\beta$ and α_{am} processes can be identified that reflects the segmental dynamics in the RAF, e.g., segments located at the crystal/amorphous interphase.[54,55] Some fitting simulations for the α_c and $\alpha\beta$ processes for the different copolymer compositions and their respective homopolymers are presented in Figure S10. At higher temperatures/lower frequencies, the dielectric loss curves for the P(VDF-TrFE) copolymers are governed by even slower processes, related to polarization effects (Maxwell–Wagner–Sillars (MWS) interfacial polarization and electrode polarization, EP)[59] (Figure S11). The dc-conductivity also contributes to the low-frequency regime of the loss curves at higher temperatures (Figure S12). Parenthetically, the *T*-dependence of the dielectric loss and the loss tangent ($\tan\delta = \varepsilon''/\varepsilon'$), obtained from isochronal scans for the same copolymer, exhibits *only* the $\alpha\beta$ and the α_c processes at lower and higher temperatures, respectively (Figure S13). This again demonstrates the importance of the frequency-dependent DS measurements.

The *T*-dependence of the relaxation times at the maximum loss for all dielectrically active processes, as well as their peak-shape parameters for three different copolymer compositions, can be discussed with the help of Figure 7 and Table S2. The figure includes TM-DSC data, depicting the two T_gs.

Starting from lower temperatures, the β process exhibits a broad distribution of relaxation times ($\langle m\rangle = 0.25 \pm 0.03$ and $\langle mn\rangle = 0.20 \pm 0.01$, for 75 mol % VDF content), reflecting heterogeneous dynamics into the glassy state. The β process has an Arrhenius temperature dependence as

$$\tau = \tau_0 \exp\left(\frac{E_a}{RT}\right) \tag{3}$$

where τ_0 is the relaxation time in the limit of very high temperatures and E_a is the activation energy. As listed in Table 2, the activation energy of the β process for the P(VDF-TrFE) copolymers is intermediate between those of the respective homopolymers. It reflects the local motion of both VDF and TrFE segments well into the glassy state. At higher temperatures, both the α_{am} and α_c processes conform to the Vogel–Fulcher–Tammann (VFT) dependence as

$$\tau = \tau_0^{\#} \exp\left(\frac{B}{T - T_0}\right) \tag{4}$$

Here, $\tau_0^{\#}$ is the relaxation time at very high temperatures, B is the activation parameter, and T_0 is the "ideal" glass temperature located below the conventional T_g. The TM-DSC data were also included in the fitting procedure of the α_{am} and the α_c processes. The VFT and Arrhenius parameters of the dielectrically active processes, as well as the values of the observed T_gs (T_g is operationally defined here as the temperature where the relaxation time is $\tau \sim 1$ s to avoid long extrapolations), are summarized in Table 2. As depicted in Figures 6, the α_c process exhibits a broader distribution ($\langle m\rangle = 0.20 \pm 0.01$ and $\langle mn\rangle = 0.20 \pm 0.01$, for 75/25 composition) and a weaker *T*-

https://doi.org/10.1021/acs.macromol.2c00280
Macromolecules 2022, 55, 2746−2757

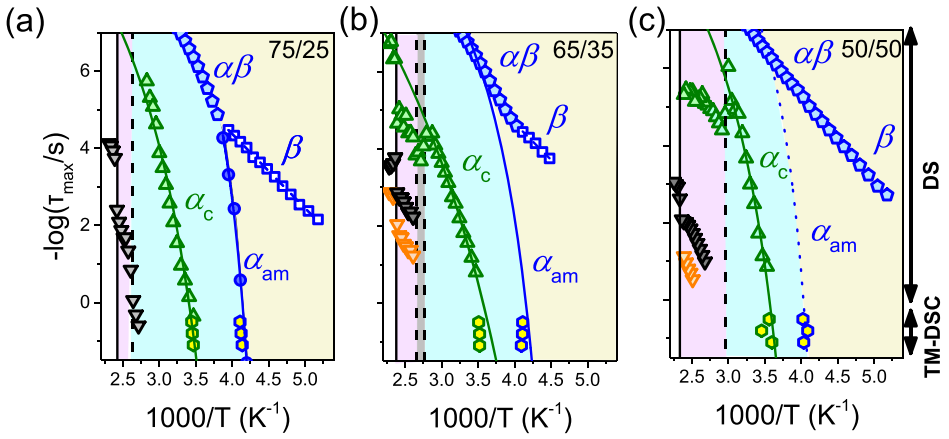

Figure 7. Relaxation times as a function of inverse temperature depicting the $\alpha\beta$ (cyan pentagons), α_{am} (blue circles), β (blue squares), and α_c (olive up-triangles) and of the slower processes associated with MWS interfacial polarization (black down triangles) and EP (orange down triangles) for the P(VDF-TrFE) copolymers with composition (a) 75/25, (b) 65/35, and (c) 50/50. All relaxation times were obtained on heating. The solid and dashed lines represent fits to a VFT and Arrhenius equations, respectively. The symbols in yellow are extracted from TM-DSC measurements. The colored areas indicate the different phases: molten state (white), PE (purple), FE or FE+DFE (cyan), temperature range of T_c (gray), and glassy state (yellow). The solid and dashed vertical lines indicate the melting and Curie temperature(s), respectively.

Table 2. VFT (Arrhenius) Parameters for the α_{am}, α_c, and β Processes of the P(VDF-TrFE) Copolymers with Different Compositions

process	VDF:TrFE ratio	$-\log(\tau_0^{\#}/s)$	B (K)	T_0 (K)	T_g (K)[a]
α_{am}	100:0	−12	970 ± 20	196 ± 1	231 ± 1
	75:25	−12	810 ± 30	212 ± 1	242 ± 1
	65:35	−12	1200 ± 100	199 ± 6	241 ± 6
	50:50	−12	810[b]	218 ± 1	248 ± 1
	0:100	−12	1620 ± 90	194 ± 4	253 ± 4
α_c	100:0	−12	4800 ± 70	113 ± 3	285 ± 3
	75:25	−12	2200 ± 100	216 ± 4	293 ± 4
	65:35	−12	3370 ± 50	158 ± 2	280 ± 2
	50:50	−12	1710 ± 90	219 ± 4	281 ± 4
	0:100	−12	2340 ± 50	196 ± 3	291 ± 3
process	VDF:TrFE ratio		$-\log(\tau_0/s)$	E_a (kJ mol^{-1})	
β	100:0		14.6 ± 0.1	46.1 ± 0.4	
	75:25		12.1 ± 0.1	36.8 ± 0.4	
	65:35		12.2 ± 0.3	36 ± 1	
	0:100		10.9 ± 0.2	32.2 ± 0.8	

[a]At $\tau \sim 1$ s. [b]Held fixed from 75/25 composition.

dependence of relaxation times in comparison to the α_{am} process ($\langle m \rangle = 0.40 \pm 0.05$ and $\langle mn \rangle = 0.25 \pm 0.02$, for 75 mol % VDF). The broad distribution within the α_c process reflects the restricted dipolar dynamics within the RAF. Furthermore, the α_c process of P(VDF-TrFE) copolymers has similar effective dielectric strength (typically, $\langle T\Delta\varepsilon \rangle = 1200 \pm 200$ K for 75/25 composition) with that of PVDF homopolymer ($\langle T\Delta\varepsilon \rangle = 1400 \pm 100$ K), implying that it reflects mainly the relaxation of VDF segments in the copolymer (Table S2). Hence, the α_{am} and α_c processes reflect mainly—but not solely—the VDF segmental dynamics within the fully amorphous and the restricted amorphous domains, respectively. The freezing temperatures of the α_{am} and α_c processes differ by about 50 K, exhibiting a small composition dependence (Figure 3).

An important finding of the present investigation is that the segmental dynamics associated with the α_c process is sensitive to the phase transformations at T_c. Specifically, its relaxation times and associated dielectric strength exhibit discontinuities at T_c, as shown in Figures 7 (Figure S14), implying a first-order transition even for a copolymer with a 50/50 composition. The influence of crossing the T_c to the slower dielectrically active processes is not evident as they are not well centered in the experimentally accessible window. As described below with respect to the P-dependent results, the discontinuity in relaxation times mainly reflects the transition from the PE to the FE + DFE phase (Figure 9). We mention here that in a recent study of porous nanofibers made of a P(VDF-TrFE) (70/30) copolymer the generated voltage reflected the relaxation of segments within the RAF phase through the α_c relaxation process.[6] Evidently, conformational changes on a time scale of 0.1 ms within the RAF hold the key for understanding the ferroelectric properties of P(VDF-TrFE) copolymers.

Exact information about the nature of T_c can be obtained by P-dependent dielectric measurements. The best candidate in this endeavor is the copolymer with the 75/25 composition followed by the 65/35 and 50/50 composition. However, in the former (75/25), the α_c relaxation times are at the border of our experimental frequency window. Therefore, to explore the effect of pressure on the molecular dynamics, we employ the copolymer with 65 mol % VDF content.

***P*-Dependence of Molecular Dynamics.** The P-dependence of relaxation times provides insight on (i) the molecular origin of dielectric processes (by using the pressure sensitivity of relaxation times and the pressure coefficient of the respective T_g's), (ii) the nature of the phase transition at T_c, and (iii) information about the stability of phases under the variation of T and P (through the $T-P$ phase diagram). Figure 8 depicts the dielectric loss curves for the P(VDF-TrFE) copolymer with 65 mol % VDF content within the FE+DFE phase by increasing pressure from 30 to 240 MPa. The P-dependence of the α_c relaxation times, corresponding to the maximum loss of the α_c process in the vicinity of T_c for the P(VDF-TrFE) copolymer with 65 mol % VDF content, is discussed with respect to Figure 9a. The relaxation times for all processes are summarized in Figure S15a.

As shown in Figures 9a (correspondingly for $\alpha\beta$, α_{am}, and α_c processes in Figure S15a), the relaxation times of α_c (and α_{am}) process follows the pressure equivalent of VFT equation as[60]

https://doi.org/10.1021/acs.macromol.2c00280
Macromolecules 2022, 55, 2746−2757

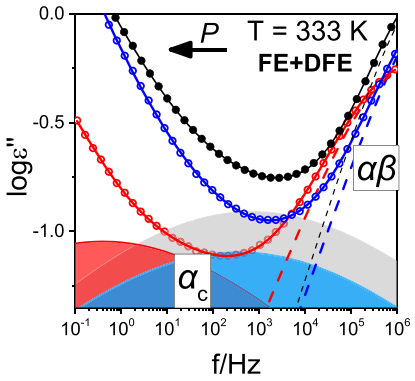

Figure 8. Dielectric loss curve for P(VDF-TrFE) copolymer as a function of frequency at T = 333 K. Pressure increases in the direction of the arrow; P = 0.1 MPa (black symbols), P = 30 MPa (blue symbols), and P = 240 MPa (red symbols). Solid lines represent fits to a summation of two HN functions in addition to the conductivity contribution. The gray, blue, and red areas (dashed lines) represent simulations of the α_c ($\alpha\beta$) process at P = 0.1 MPa, P = 30 and 240 MPa, respectively.

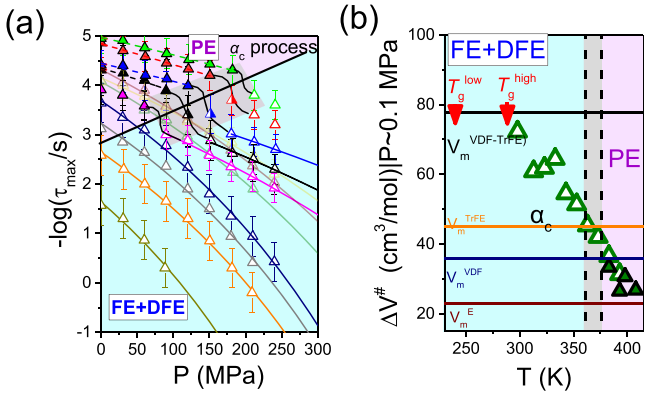

Figure 9. (a) Relaxation times as a function of pressure for the α_c process into the low-temperature FE+DFE (open symbols) at T_c (semifilled symbols) and into the high-temperature PE (filled symbols) phase for the P(VDF-TrFE) copolymer with 65/35 composition at different temperatures: 298 K (dark-yellow), 313 K (orange), 323 K (gray), 333 K (navy), 343 K (olive), 353 K (wine), 363 K (yellow), 373 K (magenta), 383 K (black), 393 K (blue), 398 K (red), and 408 K (green). The solid and dashed lines are fits to eq 5 into the FE+DFE and PE phases, respectively. The blue, gray, and purple areas indicate the FE+DFE, the pressure range of the Curie transition, and PE phase, respectively. The black diagonal line gives the approximate time at the PE to FE+DFE transition. (b) T-dependence of the apparent activation volume for the α_c (up-triangles) process into the low-temperature FE+DFE (open symbols) and into the PE (filled symbols) phase. Vertical arrows indicate the two glass temperatures. The horizontal black, orange, navy, and wine lines represent respectively the repeat unit volumes of VDF-TrFE, TrFE, VDF, and ethylene (E). The vertical dashed lines show the transitions among the weakly ordered crystalline phases. The blue, gray, and purple areas denote the FE+DFE, the temperature range of the Curie transition, and PE phases, respectively.

$$\tau_{max} = \tau_\alpha \exp\left(\frac{D_P P}{P_0 - P}\right) \tag{5}$$

where τ_α is the segmental relaxation time at atmospheric pressure at a given temperature, D_P is a dimensionless parameter, and P_0 is the pressure corresponding to the "ideal" glass. Because of the limited pressure range, the D_P value was held constant at 20 (13) for the α_c (α_{am}) process from a free fit to the 333 K (278 K) data set. The VFT parameters as a function of pressure are further provided in Table S3.

The P-dependence of relaxation times of the α_c process exhibits a discontinuity at the T_c (Figure 9a), suggesting a first-order transition. Remarkably, there is a slowing down (by about 1 order of magnitude) of the relaxation times in going from the PE to the FE phase, suggesting a higher degree of cooperativity or longer-range dynamics within the FE phase.[26] Density changes at T_c (directly linked with the change of specific volume at T_c, as discussed below) can have an impact on the slowing down of relaxation dynamics. Evidently, the PE to FE+DFE transition is not isochronal, as indicated by the slope of the block line in Figure 9a. Moreover, as depicted in Figure S15a, the slower α_c process exhibits a weaker $\tau(P)$ dependence in comparison to the α_{am} process. Parenthetically, the effect of pressure on the mixed $\alpha\beta$ process has been well-documented in the literature.[58] By increasing pressure, the $\alpha\beta$ process splits into two well-separated processes with distinctly different $\tau(P)$ dependencies.[58] On the other hand, the T-dependence of the dielectrically active processes under "isobaric" conditions is shown in Figure S15b. The α_c and α_{am} processes follow the usual VFT equation (eq 4), and the respective parameters are listed in Table S4.

The $\tau(P)$ can be employed to extract an important parameter accessible only by pressure, namely, the apparent activation volume, $\Delta V^{\#}$, corresponding to the underlying dynamic processes as[60]

$$\Delta V^{\#} = 2.303RT\left(\frac{\partial \log \tau}{\partial P}\right)_T \tag{6}$$

Earlier studies[60−64] revealed that $\Delta V^{\#}$ is coupled to the molecular volume of relaxing species. $\Delta V^{\#}$ for the α_c process has a pronounced pressure dependence ($\Delta V^{\#} = RT\frac{D_P P_0}{(P_0 - P)^2}$) (Figure S16). The extracted $\Delta V^{\#}$ at ambient pressure is plotted as a function of temperature in Figure 9b. As proposed in earlier studies,[58,61] it exhibits a strong T-dependence in the vicinity of T_g and approaches the corresponding repeat unit volume in a temperature range located some 70−90 K above T_g. Evidently, at $T \sim T_g$ + 100 K, $\Delta V^{\#}$ of the α_c process is similar to the repeat unit volume of VDF. This finding, together with the results from the T-dependent dielectric study, supports the notion that the α_c is associated with local conformational changes of the VDF segments in the constrained amorphous phase of the RAF. Moreover, at a fixed temperature, i.e., at T = 383 K (Figure 9b) where both (FE+DFE and PE) phases are present, the activation volume of the α_c process is comparable within each phase, implying a similar degree of cooperativity for the restricted amorphous phase fraction in the two phases.

The $T_c(P)$ or $P_c(T)$, as well as the $T_g(P)$, corresponding to the α_c and α_{am} processes, can be employed in the construction of the T−P phase diagram (Figure 10b). P_c was extracted from the discontinuity in the dielectric loss curves by increasing pressure under isothermal conditions (Figure 10a).

As shown in Figure 10b, T_c increases linearly with pressure and follows the Clausius−Clapeyron equation:

$$\frac{dP}{dT} = \frac{\Delta H}{T_c \Delta V} \tag{7}$$

where ΔV and ΔH are respectively the change in enthalpy and volume at the transition. The latter implies that T_c is a first-order transition. Specifically, the pressure sensitivity of T_c, dT_c/dP for

https://doi.org/10.1021/acs.macromol.2c00280
Macromolecules 2022, 55, 2746−2757

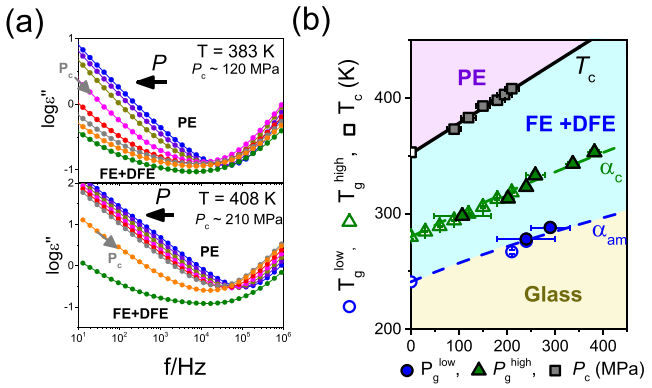

Figure 10. (a) Dielectric loss curves for the P(VDF-TrFE) copolymer with 65/35 composition as a function of frequency at (top) T = 383 K and (bottom) T = 408 K. Pressure increases in the direction of the arrow: 30 MPa (blue symbols), 60 MPa (purple symbols), 90 MPa (dark-yellow symbols), 120 MPa (magenta symbols), 150 MPa (red symbols), 180 MPa (gray symbols), 210 MPa (orange symbols), and 240 MPa (olive symbols). The P_c is also indicated with the gray arrow. (b) $P(T)$ dependence of T_c (squares) upon increasing (black symbols) compression. Glass temperatures (pressures) of the α_c (up-triangles) and α_{am} (circles) processes. The solid and dashed lines represent fits to eqs 7 and 8, respectively. The yellow, blue, purple, and red shadowed areas indicate the glass, FE+DFE, and PE phases, respectively.

the P(VDF-TrFE) copolymer with 65 mol % VDF content amounts to 263 K·GPa^{-1}. This value is lower than the one (~383 to 401 K·GPa^{-1} on heating or cooling, respectively) reported earlier[41] for a copolymer with 64.6% VDF content based on pressure-dependent permittivity values. It is also somewhat lower than the one reported from thermal expansion measurements (~318 K·GPa^{-1}) for a copolymer with 53 mol % VDF content.[42]

By employing eq 7, the change in enthalpy (ΔH = 17.8 J g^{-1}) and the Curie temperature (T_c = 372.0 K) determined by DSC measurements affords extracting the change in the specific volume at T_c. It amounts to ~0.013 cm^3 g^{-1}. This volumetric change should be compared with the one during the crystallization of the PVDF homopolymer. A 5 times larger change in specific volume (~0.06 cm^3 g^{-1})[65−67] has been reported during PVDF crystallization. This suggests that although the Curie transition is of the first order, it is accompanied by small enthalpy (volume) changes.

On the other hand, the $T_g(P)$ (the latter determined at $\tau \sim 1$ s) exhibits a nonlinear P-dependence that conforms to the following empirical equation:[68,69]

$$T_g(P) = T_g(0)\left(1 + \frac{\nu}{\mu}P\right)^{1/\nu} \quad (8)$$

Here, $T_g(0)$ is the T_g at ambient pressure, ν and μ are polymer specific parameters[60] (with values $\nu = 2.0 \pm 0.6$ (3 ± 1) and μ = 1400 ± 100 (1400 ± 80) for the α_c (α_{am}) process). Equation 8 was first proposed by Simon and Gatzel[68] for the melting of solidified gases under pressure, and subsequently, it has been employed to describe the $T_g(P)$ in glass-forming systems.[58,61,69] Specifically, the pressure coefficient of T_g^{high} (T_g^{low}) in the limit of ambient pressure, $dT_g/dP|_{P\to 0}$, is 204 K·GPa^{-1} (170 K·GPa^{-1}). Such values are typically found in low-T_g flexible polymers.[60] This is conceivable as both the low and the high T_g reflect primarily the domains of VDF segments located either in fully amorphous domains or at the crystal/amorphous interphase. To the best of our knowledge, it is the first time that the P-dependence of T_g is studied in P(VDF-TrFE) copolymers, providing additional information about the origin of the two segmental processes (α_{am} and α_c). Evidently, T_g^{high} (α_c) exhibits a somewhat stronger P-dependence, in comparison to that found for T_g^{low} (α_{am}), verifying the nature of the RAF, consisting of restricted amorphous segments.

The distinctly different P-dependence of the two T_gs with respect to the $T_c(P)$ reflects on the different thermodynamic origin of the "transitions": A kinetic arrest of the VDF segments located in amorphous configurations (low T_g) and at the crystal/amorphous interphase (high T_g) versus a weakly first-order thermodynamic phase transition at T_c. The weaker (eq 8) versus stronger (eq 7) P-dependencies of the T_gs vs T_c create an interesting situation: increasing pressure brings about a broader temperature range for the stability of the FE phase: from ~100 K at ambient pressure to ~170 K at a pressure of 350 MPa. This implies a broader temperature range for the application of P(VDF-TrFE) copolymers in ferroelectric devices.

IV. CONCLUSION

The phase behavior and the respective molecular dynamics of P(VDF-TrFE) copolymers were investigated by DSC, WAXS, and T- and P-dependent DS measurements. Coexistence of three/four *weakly ordered* phases was revealed in the vicinity of T_c, implying that P(VDF-TrFE) copolymers comprise relatively small ordered domains surrounded by large amorphous regions. Concerning the molecular dynamics, four dielectrically active processes were detected: one within the glassy state (termed as β) and three above (termed as α_{am}, $\alpha\beta$, and α_c process). Dielectric spectroscopy results unambiguously show that the α_c process is a sensitive probe of the phase transformations at T_c. Dynamical changes reflect mainly the transition from the PE to the FE + DFE phase. By employing a combination of isothermal T- and P-dependent dielectric measurements, it was shown that the α_c process reflects local conformational changes of VDF segments within the RAF, which freeze at about 50 K above the low liquid-to-glass temperature (associated with the α_{am} process). Moreover, the pressure coefficients of the liquid-to-glass temperature and of T_g^{RAF} were extracted for the first time for P(VDF-TrFE) copolymers, providing additional information about the molecular origin of the two segmental processes. In addition, P-dependent dielectric measurements provided insight into (i) the nature of the Curie transition and (ii) the stability of phases under the variation of T and P (through the T−P phase diagram). Specifically, we report that T_c increases linearly with pressure and conforms to the Clausius−Clapeyron equation, implying a first-order transition. However, the calculated change in the specific volume at T_c ($\Delta V^{\#} \sim 0.013$ cm^3 g^{-1}) is small, verifying the weak nature of the transition, as also evidenced from independent X-ray measurements. On the other hand, the two T_gs exhibit distinctly different P-dependencies with respect to T_c, reflecting on the different origin (thermodynamic vs kinetic) of the characteristic temperatures. An important finding from the T−P phase diagram is that increasing pressure brings about a broader temperature range for the stability of the FE phase. This could be an asset when designing polymer-based ferroelectric devices.

■ ASSOCIATED CONTENT

Supporting Information

The Supporting Information is available free of charge at https://pubs.acs.org/doi/10.1021/acs.macromol.2c00280.

https://doi.org/10.1021/acs.macromol.2c00280
Macromolecules 2022, 55, 2746−2757

Additional DSC and TM-DSC thermograms, WAXS patterns and dielectric data as a function of temperature and pressure for the P(VDF-TrFE) copolymer with 75 mol % VDF content and their respective homopolymers (PDF)

AUTHOR INFORMATION

Corresponding Authors

George Floudas − *Department of Physics, University of Ioannina, 451 10 Ioannina, Greece; Institute of Materials Science and Computing, University Research Center of Ioannina (URCI), 451 10 Ioannina, Greece; Max Planck Institute for Polymer Research, 55128 Mainz, Germany;* orcid.org/0000-0003-4629-3817; Email: gfloudas@uoi.gr

Kamal Asadi − *Department of Physics, University of Bath, Bath BA2 7AY, United Kingdom;* orcid.org/0000-0003-0447-4337; Email: ka787@bath.ac.uk

Author

Achilleas Pipertzis − *Department of Physics, University of Ioannina, 451 10 Ioannina, Greece*

Complete contact information is available at: https://pubs.acs.org/10.1021/acs.macromol.2c00280

Notes

The authors declare no competing financial interest.

ACKNOWLEDGMENTS

We are grateful to Saleem Anwar (MPI-P) for the film preparation used in the dielectric studies. A.P. was financially supported by the program "PERIFEREIAKI ARISTEIA" (Regional Excellence) cofinanced by the European Union and the Hellenic Republic Ministry of development and investments under NSRF 2014-2020 (Region of Epirus, call 111). This research was supported by the Hellenic Foundation for Research and Innovation (H.F.R.I.) under the "First Call for H.F.R.I. Research Projects to support Faculty members and Researchers and the procurement of high-cost research equipment grant" (Project No. 183). K.A. acknowledges the financial support from the Max Planck Institute for Polymer Research and from the University of Bath.

REFERENCES

(1) Furukawa, T.; Johnson, G. E.; Bair, H. E.; Tajitsu, Y.; Chiba, A.; Fukada, E. Ferroelectric Phase Transition in a Copolymer of Vinylidene Fluoride and Trifluoroethylene. *Ferroelectrics* **1981**, *32*, 61−67.

(2) Chen, X.; Han, X.; Shen, Q.-D. PVDF-Based Ferroelectric Polymers in Modern Flexible Electronics. *Adv. Electron. Mater.* **2017**, *3*, 1600460.

(3) Gupta, S.; Navaraj, W. T.; Lorenzelli, L.; Dahiya, R. Ultra-Thin Chips for High-Performance Flexible Electronics. *npj Flex. Electron.* **2018**, *2* (1), 8.

(4) Shirinov, A. V.; Schomburg, W. K. Pressure Sensor from a PVDF Film. *Sensors and Actuators A: Physical* **2008**, *142*, 48−55.

(5) Khanchaitit, P.; Han, K.; Gadinski, M. R.; Li, Q.; Wang, Q. Ferroelectric Polymer Networks with High Energy Density and Improved Discharged Efficiency for Dielectric Energy Storage. *Nat. Commun.* **2013**, *4*, 2845.

(6) Abolhasani, M. M.; Naebe, M.; Shirvanimoghaddam, K.; Fashandi, H.; Khayyam, H.; Joordens, M.; Pipertzis, A.; Anwar, S.; Berger, R.; Floudas, G.; Michels, J.; Asadi, K. Thermodynamic Approach to Tailor Porosity in Piezoelectric Polymer Fibers for Application in Nanogenerators. *Nano Energy* **2019**, *62*, 594−600.

(7) Lee, J.-H.; Lee, K. Y.; Kumar, B.; Tien, N. T.; Lee, N.-E.; Kim, S.-W. Highly Sensitive Stretchable Transparent Piezoelectric Nanogenerators. *Energy Environ. Sci.* **2013**, *6*, 169−175.

(8) Hu, Z.; Tian, M.; Nysten, B.; Jonas, A. M. Regular Arrays of Highly Ordered Ferroelectric Polymer Nanostructures for Non-Volatile Low-Voltage Memories. *Nat. Mater.* **2009**, *8*, 62−67.

(9) Kawai, H. The Piezoelectricity of Poy(vinylidene Fluoride). *Jpn. J. Appl. Phys.* **1969**, *8* (7), 975.

(10) Furukawa, T.; Date, M.; Fukada, E. Hysteresis Phenomena in Polyvinylidene Fluoride under High Electric Field. *J. Appl. Phys.* **1980**, *51* (2), 1135−1141.

(11) Zhang, Q. M.; Bharti, V.; Zhao, X. Giant Electrostriction and Relaxor Ferroelectric Behavior in Electron-Irradiated Poly(Vinylidene Fluoride-Trifluoroethylene) Copolymer. *Science* **1998**, *280*, 2101−2104.

(12) Furukawa, T. Ferroelectric Properties of Vinylidene Fluoride Copolymers. *Phase Transitions* **1989**, *18*, 143−211.

(13) Furukawa, T. Recent Advances in Ferroelectric Polymers. *Ferroelectrics* **1990**, *104*, 229−240.

(14) Theodoridis, A.; Papamokos, G.; Wiesenfeldt, M. P.; Wollenburg, M.; Müllen, K.; Glorius, F.; Floudas, G. Polarity Matters: Dielectric Relaxation in All-*cis*-Multifluorinated Cycloalkanes. *J. Phys. Chem. B* **2021**, *125*, 3700−3709.

(15) Tashiro, K.; Kariyo, S.; Nishimori, A.; Fujii, T.; Saragai, S.; Nakamoto, S.; Kawaguchi, T.; Maatsumoto, A.; Rangsiman, O. Development of a Simultaneous Measurement System of X-ray Diffraction and Raman Spectra: Application to Structural Study of Crystalline-phase Transitions of Chain Molecules. *J. Polym. Sci., Polym. Phys.* **2002**, *40*, 495−506.

(16) Tajitsu, Y.; Chiba, A.; Furukawa, T.; Date, M.; Fukada, E. Crystalline Phase Transition in the Copolymer of Vinylidenefluoride and Trifluoroethylene. *Appl. Phys. Lett.* **1980**, *36*, 286.

(17) Furukawa, T.; Date, M.; Fukada, E.; Tajitsu, Y.; Chiba, A. Ferroelectric Behavior in the Copolymer of Vinylidenefluoride and Trifluoroethylene. *J. Appl. Phys.* **1980**, *19*, 109.

(18) Furukawa, T.; Johnson, G. E.; Bair, E.; Tajitsu, Y.; Chiba, A.; Fukada, E. Ferroelectric Phase Transition in a Copolymer of Vinylidene Fluoride and Trifluoroethylene. *Ferroelectrics* **1981**, *32*, 61.

(19) Furukawa, T.; Johnson, G. E. Dielectric Relaxations in a Copolymer of Vinylidene Fluoride and Trifluoroethylene. *J. Appl. Phys.* **1981**, *52*, 940.

(20) Furukawa, T.; Ohuchi, M.; Chiba, A.; Date, M. Dielectric Relaxations and Molecular Motions in Homopolymers and Copolymers of Vinylidene Fluoride and Trifluoroethylene. *Macromolecules* **1982**, *17* (7), 1384−1390.

(21) Furukawa, T.; Tajitsu, Y.; Zhang, X.; Johnson, G. E. Dielectric Relaxations in Copolymers of Vinylidene Fluoride. *Ferroelectrics* **1992**, *135*, 401−417.

(22) Teyssèdre, G.; Lacabanne, C. Study of the Thermal and Dielectric Behavior of P(VDF-TrFE) Copolymers in Relation with their Electroactive Properties. *Ferroelectrics* **1995**, *171*, 125−144.

(23) Davis, G. T.; Furukawa, T.; Lovinger, A. J.; Broadhurst, M. G. Structural and Dielectric Investigations on the Nature of the Transition in a Copolymer of Vinylidene Fluoride and Trifluoroethylene (52/48 mol%). *Macromolecules* **1982**, *15*, 329−333.

(24) Tashiro, K.; Tanaka, R. Structural Correlation between Crystal Lattice and Lamellar morphology in the Ferroelectric Phase Transition of Vinylidene Fluoride - Trifluoroethylene Copolymers as Revealed by the Simultaneous measurements of Wide-angle and Small-angle X-ray Scatterings. *Polymer* **2006**, *47*, 5433−5444.

(25) Lovinger, A. J.; Davis, G. T.; Furukawa, T.; Broadhurst, M. G. Crystalline Forms in a Copolymer of Vinylidene Fluoride and Trifluoroethylene (52/48 mol%). *Macromolecules* **1982**, *15*, 323−328.

(26) Bargain, F.; Panine, P.; Domingues Dos Santos, F.; Tencé-Girault, S. From Solvent-Cast to Annealed and Polled Poly(VDF-co-TrFE) Films: New Insights on the Defective Ferroelectric Phase. *Polymer* **2016**, *105*, 144−156.

(27) Yamada, T.; Ueda, T.; Kitayama, T. Ferroelectric-to-Paraelectric Phase Transition of Vinylidene Fluoride-Trifluoroethylene Copolymer. *J. Appl. Phys.* **1981**, *52*, 948.
(28) Tashiro, K.; Kobayashi, M. Structural Phase Transition in Ferroelectric Fluorine Polymers: X-ray Diffraction and Infrared/Raman Spectroscopic Study. *Phase Transitions* **1989**, *18*, 213.
(29) Tashiro, K.; Takano, K.; Kobayashi, M.; Chatani, Y.; Tadokoro, H. Structural Study on Ferroelectric Phase Transition of Vinylidene Copolymers Fluoride Trifluoroethylene Copolymers (III) Dependence of Transitional Behavior on VDF Molar Content. *Ferroelectrics* **1984**, *57*, 297−326.
(30) Hirose, R.; Yoshioka, T.; Yamamoto, H.; Reddy, K. R.; Tahara, D.; Hamada, K.; Tashiro, K. In-house Simultaneous Collection of Small-angle X-ray Scattering, Wide-angle X-ray Diffraction and Raman Scattering Data from Polymeric Materials. *J. Appl. Crystallogr.* **2014**, *47*, 922−930.
(31) Liu, Y.; Aziguli, H.; Zhang, B.; Xu, W.; Lu, W.; Bernholc, J.; Wang, Q. Ferroelecrric Polymers Exhibiting Behavior Reminiscent of a Morphotropic Phase Boundary. *Nature* **2018**, *562*, 96−100.
(32) Liu, Y.; Han, Z.; Xu, W.; Haibibu, A.; Wang, Q. Composition-Dependent Dielectric Properties of Poly(vinylidene Fluoride-trifluorooethylene)s Near the Morphotropic Phase Boundary. *Macromolecules* **2019**, *52*, 6741−6747.
(33) Liu, Y.; Zhang, B.; Haibibu, A.; Xu, W.; Han, Z.; Lu, W.; Bernholc, J.; Wang, Q. Insights into the Morphotropic Phase Boundary in Ferroelectric Polymers from the Molecular Perspective. *J. Phys. Chem. C* **2019**, *123*, 8727−8730.
(34) Ng, C.Y. B.; Gan, W. C.; Velayutham, T. S.; Goh, B. T.; Hashim, R. Structural Control of Dielectric, Pyroelectric and Ferroelectric Properties of Poly(vinylidene Fluoride-co-Trifluoroethylene) Thin Films. *Phys. Chem. Chem. Phys.* **2020**, *22*, 2414−2423.
(35) Septiyani Arifin, D. E.; Ruan, J J Study on the Curie Transition of P(VDF-TrFE) Copolymer. *IOP Conf. Ser.: Mater. Sci. Eng.* **2018**, *299*, 012056.
(36) Kim, K. J.; Kim, G. B.; Vanlencia, C. L.; Rabolt, J. F. Curie Transition, Ferroelectric Crystal Structure, and Ferroelectricity of a VDF/TrFE (75/25) Copolymer. 1. The Effect of the Consecutive Annealing in the Ferroelectric State on Curie Transition and Ferroelectric Crystal Structure. *J. Polym. Sci., Part B: Polym. Phys.* **1994**, *32*, 2435−2444.
(37) Teyssedre, G.; Bernes, A.; Lacabanne, C. Cooperative Movements Associated with the Curie Transition in P(VDF-TrFE) Copolymers. *J. Polym. Sci., Part B: Polym. Phys.* **1995**, *33* (6), 879−890.
(38) Mizuno, H.; Nagano, Y.; Tashiro, K.; Kobayashi, M. A Study of the Ferroelectric Phase Transition of Vinylidene Fluoride-Trifluoroethylene Copolymers by ac Calorimetry. *J. Chem. Phys.* **1992**, *96*, 3234−3239.
(39) Ohigashi, H.; Hattori, T. Improvement of Piezoelectric Properties of Poly(vinylidene Fluoride) and its Copolymers by Crystallization under High Pressures. *Ferroelectrics* **1995**, *171*, 11−32.
(40) Hattori, T.; Hikosaka, M.; Ohigashi, H. The Crystallization Behavior and Phase Diagram of Extended-chain Crystals of Poly-(vinylidene fluoride) under High Pressure. *Polymer* **1996**, *37*, 85−91.
(41) Koizumi, N.; Haikawa, N.; Habuka, H. Dielectric Behavior and Ferroelectric Transition of Copolymers of Vinylidene Fluoride and Trifluoroethylene. *Ferroelectrics* **1984**, *57*, 99−119.
(42) Koizumi, N.; Murata, Y.; Oka, Y. Pressure Dependence of Ferroelectric Transition and Anomaly in Bulk Modulus in Copolymer of Vinylidene Fluoride and Trifluoroethylene. *Jpn. J. Appl. Phys.* **1984**, *23*, 324−326.
(43) Serghei, A.; Zhao, W.; Miranda, D.; Russell, T. P. Curie Transitions for Attograms of Ferroelectric Polymers. *Nano Lett.* **2013**, *13*, 577−580.
(44) Bargain, F.; Thuau, D.; Panine, P.; Hadziioannou, G.; Domingues Dos Santos, F.; Tence-Girault, S. Thermal Behavior of Poly(VDF-ter-TrFE-ter-CTFE) Copolymers: Influence of CTFE termonomer on the Crystal-crystal Transitions. *Polymer* **2019**, *161*, 64−77.
(45) Weiss, R. J. The Origin of the 'Invar' effect. *Proc. Phys. Spc.* **1963**, *82*, 281−288.
(46) Wei, S.; Duraj, R.; Zach, R.; Matsushita, M.; Takahashi, A.; Inoue, H.; Ono, F.; Maeta, H.; Iwase, A.; Endo, S. The Effect of Pressure on the Curie Temperature in Fe-Ni Invar Mechanical Alloys. *J. Phys.: Condens. Matter* **2002**, *14*, 11081.
(47) Wunderlich, B.; Jin, Y.; Boller, A. Mathematical Description of Differential Scanning Calorimetry Based on Periodic Temperature Modulation. *Thermochim. Acta* **1994**, *238*, 277−293.
(48) Simon, S. Temperature-Modulated Differential Scanning Calorimetry: Theory and Application. *Thermochim. Acta* **2001**, *374*, 55−71.
(49) Hensel, A.; Dobbertin, J.; Schawe, J. E. K.; Boller, A.; Schick, C. Temperature-Modulated Calorimetry and Dielectric Spectroscopy in the Glass Transition Region of Polymers. J. *Therm. Anal.* **1996**, *46*, 935−954.
(50) Floudas, G. Effects of Pressure on Systems with Intrinsic Orientational Order. *Prog. Polym. Sci.* **2004**, *29*, 1143−1171.
(51) Kremer, F.; Schönhals, A. *Broadband Dielectric Spectroscopy*; Springer: Berlin, 2002.
(52) Floudas, G. Dielectric Spectroscopy. In *Polymer Science: A Comprehensive Reference*; Matyjaszewski, K., Möller, M., Eds.; Elsevier BV: Amsterdam, 2012; Vol. 2.32, pp 825−845.
(53) Havriliak, S.; Negami, S. A complex Plane Representation of Dielectric and Mechanical Relaxation Processes in Some Polymers. *Polymer* **1967**, *8*, 161−210.
(54) Wunderlich, B. Reversible Crystallization and the Rigid - Amorphous Phase in Semicrystalline Macromolecules. *Prog. Polym. Sci.* **2003**, *28*, 383−450.
(55) Dimitriadis, T.; Bikiaris, D. N.; Papageorgiou, G. Z.; Floudas, G. Molecular Dynamics of Poly(ethylene - 2,5 - furonoate) (PEF) as a function of the degree of Crystallinity by Dielectric Spectroscopy and Calorimetry. *Macromol. Chem. Phys.* **2016**, *217*, 2056−2062.
(56) Donth, E. The Size of Cooperatively Rearranging Regions at the Glass Transition. *J. Non-Cryst. Solids* **1982**, *53*, 325−330.
(57) Simoes, R. D.; Rodriguez-Perez, M. A.; De Saja, J. A.; Constantino, C. J. L. Tailoring the Structural Properties of PVDF and P(VDF-TrFE) by Using Natural Polymers as Additives. *Polym. Eng. Sci.* **2009**, *49* (11), 2150−2157.
(58) Mpoukouvalas, K.; Floudas, G.; Williams, G. Origin of the α, β, ($\beta\alpha$), and "Slow" Dielectric Processes in Poly(ethyl methacrylate). *Macromolecules* **2009**, *42* (13), 4690−4700.
(59) Samet, A.; Levchenko, V.; Boiteux, G.; Seytre, G.; Kallel, A.; Serghei, A. Electrode Polarization vs. Maxwell-Wagner-Sillars Interfacial Polarization in Dielectric Spectra of Materials: Characteristic frequencies and scaling laws. *J. Chem. Phys.* **2015**, *142*, 194703.
(60) Floudas, G.; Paluch, M.; Grzybowski, A.; Ngai, K. *Molecular Dynamics of Glass-Forming Systems: Effects of Pressure*; Springer Science & Business Media: 2010; Vol. *1*.
(61) Floudas, G.; Gravalides, C.; Reisinger, T.; Wegner, G. Effect of Pressure on the Segmental and Chain Dynamics of Polyisoprene. Molecular weight dependence. *J. Chem. Phys.* **1999**, *111*, 9847.
(62) Floudas, G.; Reisinger, T. Pressure Dependence of the Local and Global Dynamics of Polyisoprene. *J. Chem. Phys.* **1999**, *111*, 5201.
(63) Floudas, G.; Fytas, G.; Reisinger, T.; Wegner, G. Pressure induced Dynamic Homogeneity in an Athermal Diblock Copolymer Melt. *J. Chem. Phys.* **1999**, *111*, 9129−9132.
(64) Paluch, M.; Grzybowska, K.; Grzybowski, A. Effect of High Pressure on the Relaxation Dynamics of Glass-forming Liquids. *J. Phys.: Condens. Matter* **2007**, *19*, 205117.
(65) Mekhilef, N. Viscoelastic and Pressure-Volume-Temperature Properties of Poly(vinylidene fluoride) and Poly(vinylidene fluoride)-Hexafluoropropylene Copolymers. *J. Appl. Polym. Sci.* **2001**, *80* (2), 230−241.
(66) Rodgers, P. A. Pressure-Volume-Temperature Relationships for Poly(vinylidene fluoride) and Polyamide-11. *J. Appl. Polym. Sci.* **1993**, *50*, 2075−2083.
(67) Zoller, P.; Walsh, D. *Standard Pressure-Vol.-Temperature Data for Polymers*; Technomic Publishing: Lancaster, PA, 1995.

https://doi.org/10.1021/acs.macromol.2c00280
Macromolecules 2022, 55, 2746−2757

(68) Simon, F. E.; Glatzel, Z. Z. Anorg. *Allg. Chem.* **1929**, *178*, 309.
(69) Andersson, S. P.; Andersson, O. Relaxation Studies of Poly(propylene glycol) under High Pressure. *Macromolecules* **1998**, *31*, 2999.

https://doi.org/10.1021/acs.macromol.2c00280
Macromolecules 2022, 55, 2746−2757